PARTICLE AGGREGATE GROWTH IN AN ULTRASOUND STANDING WAVE TRAP

W. T. Coakley, D. Bazou and J. F. Spengler
Cardiff School of Biosciences, Cardiff University, U.K.
coakley@cf.ac.uk

Abstract

Growth of 2-dimensional aggregates of 25 μm diameter latex particles in water and in solutions of $CaCl_2$ has been examined in an ultrasound standing wave trap (USWT) that draws microparticles from suspensions into a video-microscope pre-focused central region of the pressure node plane. The ultrasound chamber had a single half wavelength pathlength at its resonant frequency of 3.17 MHz. Aggregate growth of 25 μm latex, was monitored. The fractal (perimeter) dimension of aggregates ranged from 1.14 in deionised water to 1.58 in 20 mM salt. These values were consistent with predictions for reaction limited aggregation (RLCA) and diffusion limited aggregation (DLCA) in the control and high calcium concentration samples respectively. 'Cross-over' behaviours intermediate between those for the two limiting situations were observed as the salt concentration increased. The acoustic particle interaction forces are small compared to the forces that normally control microparticle aggregation. It is concluded that the non-intrusive USWT has potential for elucidating aggregate growth patterns.

Introduction

Aggregation in colloidal suspensions governs many processes in the chemical, environmental, biotechnological, pharmaceutical and food industries. The probability of the particles sticking upon contact is a fundamental factor that leads to two universal limiting aggregation regimes. In the first, diffusion limited colloid aggregation (DLCA), particles bind upon contact while in the second, reaction limited aggregation (RLCA), a repulsive barrier limits the efficiency of collisions. The insights on coagulation kinetics, internal dynamics and annealing processes, to be obtained from study of 2-dimensional aggregation of microparticles trapped by surface tension at the interface between air and water have been recognised for many years [1]. The ultrasonic standing wave trap (USWT) approach to aggregate characterisation employed here retains the advantages of real time optical microscopy while freeing the system from the constraints imposed at air-water interfaces.

The axial radiation force DRF_a that drives spheres of volume V, density ρ_p and compressibility β_p to a node or antinode plane in a liquid of density ρ_o and compressibility β_o, is given by

$$DRF_a = -\pi P_o^2 V \beta_o/(2\lambda).\phi(\beta,\rho).\sin(4\pi z/\lambda) \qquad (1)$$

where P_o is the sound pressure amplitude, z is distance from a pressure node, and λ is the wavelength of the driving frequency in water. The contrast factor ϕ is

$$\phi(\beta,\rho) = (5\rho_p - 2\rho_o)/(2\rho_p + \rho_o) - \beta_p/\beta_o \qquad (2)$$

Latex microparticles, for which ϕ is positive, move towards the pressure node plane. They then move towards and accumulate at preferred positions within the node plane. This in-plane movement has been attributed to a lateral radiation force (DRF_l), that is of the same origin as DRF_a, but is smaller in magnitude [2, 3], and to convective Rayleigh-scale streaming [3]. The morphology and stability of latex microsphere aggregates formed in an USWT in deionised water and where electrostatic repulsion of particles has been modified by suspension in $CaCl_2$ are described here. The form of the aggregates had been characterised by a perimeter fractal dimension. The magnitudes of the attractive acoustic particle interactions are compared with the relatively short-range colloidal particle interactions that normally influence aggregate morphology. The results suggest that the ultrasound trap does not modify reaction-determined contributions to aggregate growth in the systems tested.

Materials and Methods.

Ultrasonic trap. The three main components of the USWT were the transducer, the spacer and the reflector. The electrodes of a 3×3 cm^2 transducer (Ferroperm, Denmark) were etched to give a 10×10 mm^2 top electrode and a circular (6 mm diameter) back electrode. This geometry resulted in a single 'central' aggregate at the axis of the chamber. The 0.25 mm thick spacer was one $\lambda/2$ in water (at the chamber resonant frequency). The $3\lambda/4$ thick (1.48 mm) quartz acoustic reflector provided optical access to the chamber. A sine input (33120A, Hewlett Packard) to an RF amplifier (ENI 2100L, ENI Rochester, NY) was controlled by computerised tracking of a transducer voltage-maximum frequency [4] of about 3.17 MHz

Experimental procedure, microscopy and image analysis. 25 μm diameter polystyrene latex particles (Polymer Laboratories) were prepared as 0.15% solids, unless otherwise stated, in a volume of 20 ml. They were suspended in deionised water or in 2, 4, 8, 10 and 20 mM $CaCl_2$ solutions. Figure 1 shows the experimental set-up. The microscope was pre-focused on the central area in the pressure nodal plane.

Suspension was pumped (Gilson minipuls3) into the chamber. Video recording and sonication began shortly after the pump was switched off (batch mode). Observation in the direction normal to the transducer was performed with an Olympus BX 40 reflection microscope. Video sequence recording onto tape and PC by a PAL CCD camera (Fujitsu) has previously been described [4]. Images were imported as .tif files into Adobe Photoshop 5.5 and filter routines were employed for automatic analysis. The perimeter fractal dimension of aggregates formed under varied conditions in USWT was determined.

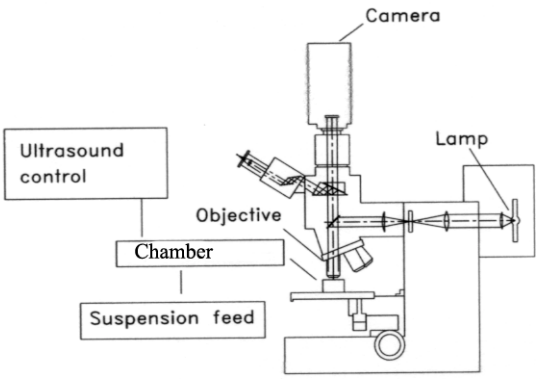

Fig. 1. Schematic diagram of the experimental assembly: The standing wave chamber is on the microscope stage.

Results

The latex particles in deionised water all reached the pre-focused nodal plane, as single particles, within 2 video frames of applying ultrasound (Fig. 2a). Single particles and some small clusters approach the central aggregate that had developed by 5 s (Fig. 2b). Generally larger clusters (usually formed and moving in from outside the field of view) and a few single particles were approaching the growing aggregate at 15 s. A clear ordered structure has by then formed in the central aggregate (Fig. 2c). Video observations showed that the single particles and clusters rolled, within the node plane, about the edge particles as they merged with the central aggregate. The large scale of the regions of order within the central aggregate confirms that the incorporation of clusters was accommodated by rearrangement of the individual particles into a close packed pattern (Fig. 2d). It follows that aggregation out of the stable suspension in deionised water is an extreme case of the RLCA regime, where the reaction kinetic is so slow that no permanent particle-particle contact is formed (collision efficiency is 0).

Sequences of an aggregate growing in 10 mM $CaCl_2$ are shown in Figure 3. Particles adhered permanently at the first contact. The inflowing small clusters (Fig. 3b) formed a central aggregate. No merging or rearrangement was observed following cluster-cluster contact. As the dendritic structure 'backbone' grew (Fig. 3c) some folding took place, as was also the situation when long clusters joined the main aggregate. The typical outcome was an open dendritic structure as in Figure 3d. This is typical of DLCA where, since the collision efficiency is 1, the transport of particles to each other is the limiting step in forming aggregates.

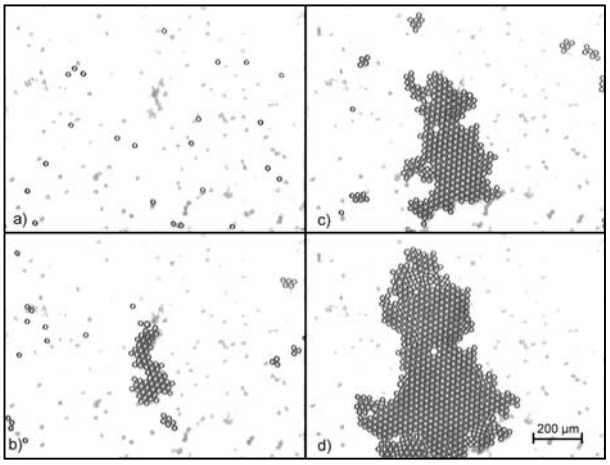

Fig. 2 Development of an aggregate of 25 µm latex particles (0.15 % solids) in deionised water at time; (a) t = 0.08 s, all particles are in focus in nodal plane; (b) 5 s, (c) 15 s, (d) 30 s. P_o was 0.5 MPa [5].

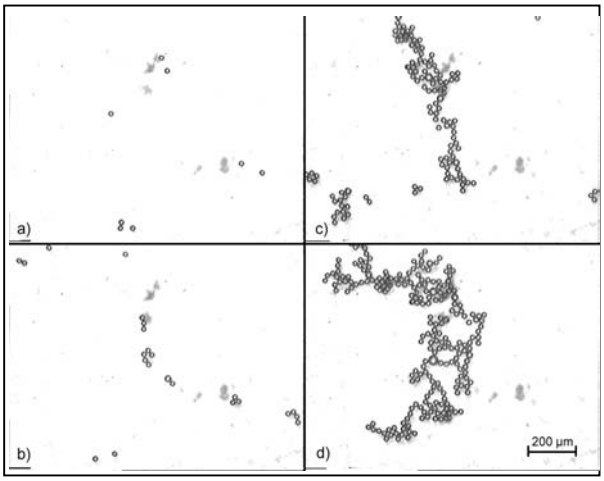

Fig. 3 Development of particle (0.075% solids) aggregate in 10 mM $CaCl_2$; (a) t = 0.08 s, particles in focus in the nodal plane; (b) 5 s, (c) 15 s, (d) 30 s. P_o was 0.5 MPa [5].

The ability of particles to form permanent contacts increased with increasing calcium concentration, resulting in aggregates with more and more open dendritic structures. A decrease in the ability of the aggregate to rearrange itself was also apparent as salt concentration was increased. The aggregation process was almost complete after 40 s as few free particles were left in the microscope field of view (Fig. 4). The fractal dimensions of duplicate series of 25 µm latex

aggregates formed in increasing electrolyte concentrations are shown in Figure 5. The analysis was performed on the final aggregate images.

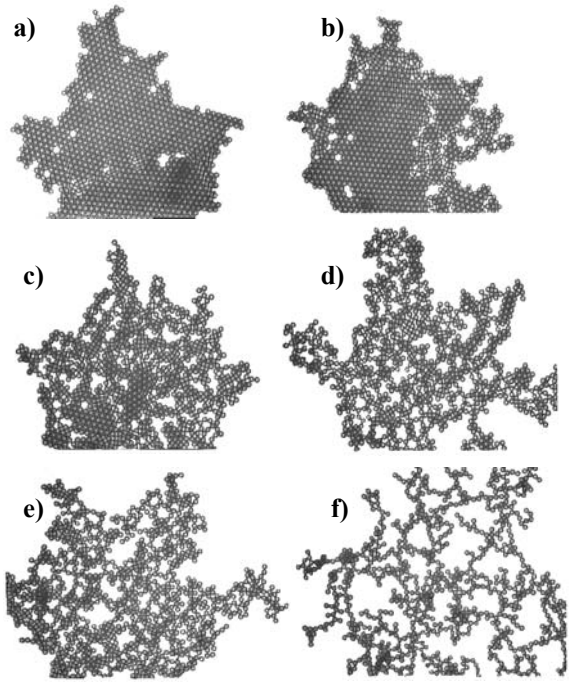

Fig. 4 25 µm latex aggregates formed after 40 s at the pressure node in 0 (a), 2 (b), 4 (c), 8 (d), 10 (e) and 20 (f) mM [$CaCl_2$] P_o was 0.27 MPa.

Discussion.

The technique delivered the 25 µm particles into the microscope focal plane, that had been preset to coincide with an acoustic pressure node plane, within two frame times of initiation of exposure. The time *t* for all particles of initial distance z_1 ($z_1 < \lambda/4$) or less from the nodal plane to be moved, under radiation force alone, within a distance of z_2 from the node plane is given [6] by

$$t = (3\lambda^2 \eta r / \pi).[1n(\tan(2\pi z / \lambda)]_{z1}^{z2} /[P_0^2 V \beta_w . \phi(\beta, \rho)] \quad (3)$$

where η is the viscosity of water and *r* is the radius of the particle. The distance from the pressure node to the reflector or transducer ($\lambda/4$) in this work is approximately 125 µm. Since the centre of mass of a 25 µm particle at the transducer wall is 12.5 µm from that wall we can obtain an estimate, of the time for some part of all particles to lie in the node plane. The resulting time estimate, when P_o = 0.5 Mpa, is 19 ms. The time is consistent with the observation of all particles being in the focal plane within two video frames (< 80 ms) of exposure to ultrasound. It follows that the clustering recorded as the particles moved towards a central aggregation region, occurred in 2-D. The final aggregate had a single-layer '2-dimensional' geometry.

The fractal perimeter dimension employed here has a value of 1.0 for a closed, circular compact aggregate whereas more dendritic structures have values tending to an upper limit of 2. The RLCA model predicts than articles do not permanently attach on contact (low collision efficiency) and thus rearrange to form packed aggregates. This description applies to aggregates formed in deionised water and approximates the 2 and

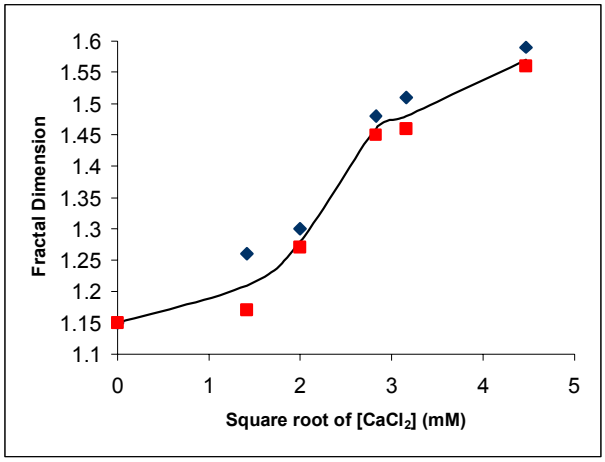

Fig. 5 [$CaCl_2$] dependence of the fractal index of replicate latex aggregates. Data are plotted against $[CaCl_2]^{0.5}$, since the square root of ionic strength is proportional to the reciprocal of the Debye length (an index of the range of electrostatic repulsion).

4 mM [$CaCl_2$]) situations. The DLCA model describes the aggregation processes when every contact between two surfaces leads to a permanent attachment (collision efficiency factor of 1). Such aggregates exhibit an open structure. The aggregates formed here at 8, 10 and 20 mM [$CaCl_2$] are consistent with the DLCA model.

The above models, need to be considered together, as a single approach cannot describe the real aggregation phenomenon extensively and more importantly cannot fully describe the gradual crossover from the RLCA to the DLCA model [7] that occurs in our experiments between 4 and 8 mM [$CaCl_2$]. Fractal dimension measurements confirm that the transitions are centred around a $CaCl_2$ concentration of 6 mM (Fig. 5).

Forces on test particles.

A physical trap employed to quantify fractal dimension should be non-intrusive so as not to modify the probability that particles will stick on contact. The ultrasonic interaction forces are quantified below and compared with the influence of factors such as the van der Waals interaction and electrostatic repulsion normally considered in assessing suspension stability. The density-dependent interactive force between two rigid spheres of equal size may be described [8] by

radial-coordinate components, $F_{\rho r}$ and $F_{\rho\phi}$, in the direction of the line connecting the particle centres and in the direction of the angle ϕ between the lines connecting the particle centres and the direction of fluid movement in the absence of particles respectively. The components are,

$$F_{\rho r} = 2\pi(\rho_p - \rho_o)^2.(P_o/\rho_o c_o)^2.r^6/[3\rho_o(2r + h)^4].$$
$$(3\cos^2\phi - 1) \qquad (4a)$$

$$F_{\rho\phi} = - 2\pi(\rho_p - \rho_o)^2.(P_o/\rho_o c_o)^2.r^6/[3\rho_o(2r + h)^4].$$
$$(\sin 2\phi) \qquad (4b)$$

For two adjacent particles in the pressure node plane ($\phi = \pi/2$) $F_{\rho\phi}$ is zero while $F_{\rho r}$ is attractive and equal to $2\pi(\rho_p-\rho_o)^2.(P_o/\rho_o c_o)^2.r^6/[3\rho_o(2r+h)^4]$.(For the situation obtaining here r is 12.5 μm and h, for typical surface separations, is taken to be of the order of 10 nm). $F_{\rho r}$ may then be approximated by

$$F_{\rho r} = - 2\pi(\rho_p - \rho_o)^2.(P_o/\rho_o c_o)^2.r^6/[3\rho_o(2r)^4]. \qquad (5)$$

The force is 7.2 pN when P_o = 1 MPa, ρ_p = 1,056 kg m^{-3}, and c_o = 1,480 m s^{-1}. The compressibility-dependent attractive inter-particle force F_β on spheres suspended in a standing wave decreases to zero as particles reach the pressure node [4].

The attractive van der Waals interaction between the two equal sized spheres of radius r and nearest center to center approach of 2r+h may be approximated, for r >> h, by

$$F_w = - Ar/(12h^2) \qquad (6)$$

where A is the Hamaker constant. A is $2.2\text{x}10^{-20}$ J for polystyrene. The attractive acoustic force and the van der Waals force are equal in magnitude when h = 57 nm. The van der Waals force then becomes increasingly more important for smaller values of h. It is reasonable to assume that attenuation of electrostatic repulsion is the factor controlling the change in aggregate morphology in the experiments reported above. The distance κ^{-1} over which electrostatic repulsion between charged particles in an electrolyte of ionic strength I is attenuated by a factor of e is given by, $\kappa^{-1} = 4.31\text{x}10^{-10}(2I)^{-0.5}$ m. For 10 mM $CaCl_2$ (I = 0.03), κ^{-1} = 1.76 nm. This distance is very small compared to the separation of 57 nm below which acoustic attraction becomes smaller than the van der Waals force. It follows, that for the particles considered here, acoustic interaction does not make a significant contribution to the forces that determine the surface-surface interactions controlling aggregate morphology and collision efficiency.

Conclusions

The technique described provides a novel approach to the formation of 2-D particle aggregates. While it retains the general information-extraction merits seen for 2-D systems aggregating at air-water interfaces [1] it removes the requirement to modify expressions for particle interactions because of the location of particles at interfaces [1]. Since the acoustic contrast factor (Eq. 2) is similar in magnitude for latex and/or human erythrocytes the techniques has potential for study of the general progression of cell adhesion in suspension.

Acknowledgements:

JFS was supported by EU-TMR contract No. ERBFMRXCT97-0156 UltraSonoSep.

References

[1] R. Hidalgo-Álvarez, A. Martín, A. Fernández, D. Bastos, F. Martínez, F.J. de las Nieves, "Electrokinetic properties, colloidal stability and aggregation kinetics of polymer colloids," Adv. Colloid Interface Sci., vol. 67, pp.1-118, 1996.

[2] S.M. Woodside, B.D. Bowen, J.M. Piret, "Measurements of ultrasonic forces for particle-liquid separations," AIChE J., vol. 43, pp. 1727-1736, 1997.

[3] J.F. Spengler, W.T. Coakley, K.T. Christensen, "Microstreaming effects on particle concentration in an ultrasonic standing wave," AIChE J., in press. 2003.

[4] J.F. Spengler, M. Jekel, K.T. Christensen, R.J. Adrian, J.J. Hawkes, W.T. Coakley, "Observation of yeast cell movement and aggregation in a small-scale MHz-ultrasonic standing wave field," Bioseparation, vol. 9, pp. 329-341. 2001.

[5] J.F. Spengler, W.T. Coakley, "Ultrasonic trap to monitor morphology and stability of developing microparticle aggregates," Langmuir, vol. 19, pp. 3635-3642. 2003.

[6] M.S. Limaye, W.T. Coakley. Clarification of small volume microbial suspensions in an ultrasonic standing wave. J. Appl. Microbiol., vol. 84, pp. 1035-1042. 1998.

[7] D. Asnaghi, M. Carpinetti, M. Giglio, M. Sozzi. Coagulation kinetics and aggregate morphology in the intermediate regimes between diffusion-limited and reaction-limited cluster aggregation. Phys. Rev. A, vol. 45, pp. 1018-1023. 1992.

[8] W.L. Nyborg, Ultrasound: its application in medicine and biology; Fry, F. J. Ed.; vol. 1, p 1. Elsevier, Amsterdam, 1978.